Pattern Recognition 45 (2012) 934–946

Contents lists available at SciVerse ScienceDirect

Pattern Recognition

journal homepage: www.elsevier.com/locate/pr

Dental biometrics: Human identification based on teeth and dental works in bitewing radiographs

Phen-Lan Lin [a], Yan-Hao Lai [b], Po-Whei Huang [b,*]

[a] Department of Computer Science and Information Engineering, Providence University, Shalu, Taichung 43301, Taiwan, ROC
[b] Department of Computer Science and Engineering, National Chung Hsing University, 250 Kuo Kuang Rd., Taichung 40227, Taiwan, ROC

ARTICLE INFO

Article history:
Received 7 January 2011
Received in revised form
27 August 2011
Accepted 30 August 2011
Available online 7 September 2011

Keywords:
Bitewing radiographs
Dental identification
Postmortem identification
Dental work matching
Tooth matching

ABSTRACT

This paper presents an enhanced dental identification method based on both the contours of teeth and dental works. To reduce the alignment error caused from unreliable contours, we propose a point-reliability measuring method and weigh each point based on its reliability when calculating the Hausdorff distance (HD) between the contours. For reducing the alignment error caused from incomplete tooth contours, we propose an outlier detection method to prune the outliers from each contour and realign the pruned contours. And for compensating the error when matching with the spatial feature of dental works due to imperfect alignment of the teeth in which they reside, we propose using an additional alignment-invariant frequency feature of dental works. Experimental results show that our method can achieve (1) 94.3% and 100% image retrieval accuracy of the top-1 and -5 retrievals, respectively, when matching with the weighted HD for the pruned contour of a single tooth; (2) 100% accuracy of top-2 (top 6%) image retrievals when matching with both contours of teeth and dental works.

1. Introduction

Biometrics is an identification technology for uniquely recognizing individuals based on measuring the subject's physical or behavioral traits, such as fingerprint, iris, and voice. According to a survey report [1], the market of biometrics is growing rapidly and more commercial products for access control, transaction security, and law enforcement are available each year.

In the law enforcement sector, "forensic identification may take place prior to death and is referred to as Antemortem (AM) identification. Identification may as well be carried out after death and is called Postmortem (PM) identification" [2]. Most of the behavioral and physiological traits are not suitable for PM identification when the victims are under severe decaying of soft tissues or mass disasters such as fire or collision. Teeth, being the hardest and the most impregnable part of human body, are thus regarded as the best candidate for PM identification [3].

In traditional dental identification, forensic odontologists manually compare PM dental radiographs with all of AM dental radiographs stored in the database using distinctive features such as dental restoration, dental work, morphology of root, and teeth. Such work is time consuming and often not good enough to correctly identify individuals. For more efficient and accurate identification, some Automatic Dental Identification Systems (ADIS) [4–6], which involve teeth segmentation, teeth classification, teeth numbering, and human identification, had been proposed to search the AM database for the best matches to a given PM dental radiograph.

Many methods of human identification that mainly used tooth contours as the matching feature had been reported in literature [4,5,7,8]. However, using tooth contours as the only feature in dental identification is not always reliable due to several challenges [9]: (1) Poor quality of radiographs, which will influence the precision of teeth segmentation and consequently affect the matching accuracy. (2) Changes of tooth shape over time, which will lead to the difficulty in matching with AM radiographs. (3) View variance of radiographs, which will result in a non-linear deformation of images and influence the precision of alignment. (4) Small interclass variation, which will produce very similar features in the same category from different individuals due to that dental radiographs are 2D projection of 3D objects [6]. Fig. 1(a) and (b) are two dental radiographs of the same person acquired in the year 2003 and 2008, respectively. We can notice that the tooth shapes become different after a long time (especially in bicuspid) and appear deformed in different views.

On the other hand, dental works (DWs), such as crown, bridge, and filling as shown in Fig. 1(c)–(f), usually appear brighter than

* Corresponding author. Tel.: +886 4 2285 1528; fax: +886 4 2285 3870.
E-mail addresses: lan@pu.edu.tw (P.-L. Lin), yanhao.lai@gmail.com (Y.-H. Lai), powhei.huang@msa.hinet.net (P.-W. Huang).

0031-3203/$ - see front matter © 2011 Elsevier Ltd. All rights reserved.
doi:10.1016/j.patcog.2011.08.027

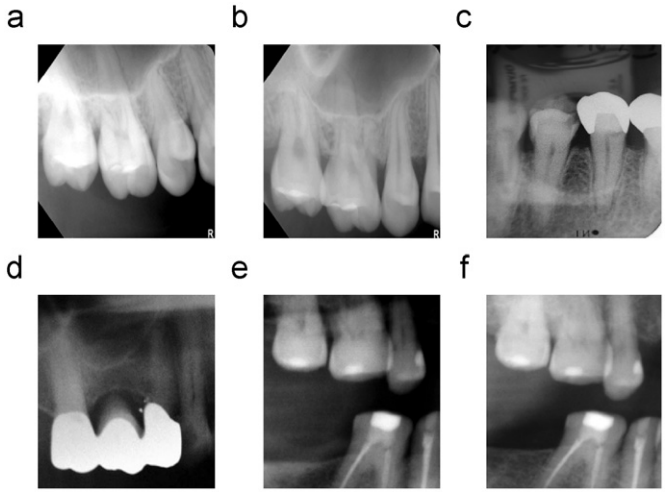

Fig. 1. Examples of dental radiographs acquired in different years. (a) From person-1 in 2003. (b) From person-1 in 2008. (c) Dental work-crown (d) Dental work-bridge. (e),(f) Dental work-filling (from person-2 in 2005 and 2009, respectively).

teeth, and their contours are not as noisy as tooth contours. Meanwhile, DWs are not sensitive to view variation and shape change over time, as shown in Fig. 1(e) and (f), which are the radiographs from the same person captured in the year 2005 and 2009, respectively. Thus, DWs can be used as another salient feature for dental matching. Chen and Jain [10] utilized an area-based metric for matching the dental works, and then fused both the similarity measurements of tooth contours and dental works to improve identification accuracy. Hofer and Marana [11] presented a dental identification method based on the information of all DWs in the image, including position, size, and distance between neighboring DWs. However, using spatial domain features for dental matching relies heavily on teeth alignment. Incorrect matching can occur when two tooth contours are either unreliable due to poor image quality or not both completely available due to images taken in rather different angles, which causes unsatisfactory alignment.

Dental features other than tooth contour point set and dental works had also been investigated. Nomir and Abdel-Mottaleb proposed a signature vector containing salient points that are tooth contour points with high curvature [5]. However, they found that such feature was not robust enough against poor quality image. They later proposed another type of salient points based on teeth appearance to overcome the poor quality image problem [12]. The method exploited the forcefield formed from the teeth appearance to locate a small number of potential energy wells as the saliency points. Their experimental results showed that using the forcefield-based feature did not outperform the Fourier descriptors of tooth contour for teeth matching or alignment; however, the accuracy can indeed be improved by combining both features.

According to the view and coverage, the most commonly used dental radiographs are panoramic, periapical, and bitewing. Panoramic has complete upper and lower jaws, but has little fine detailed teeth information. Periapical, on the other hand, shows the entire view of specific teeth, including crowns and roots, but it always has few teeth. Bitewing presents the crowns and parts of the roots of molar and pre-molar teeth, which are more distinctive than other teeth.

In this paper, we present an enhanced dental identification method based on both the contours of teeth and dental works. For reducing the alignment error caused from unreliable contours, we propose weighing each contour point based on its reliability when calculating the distance between two contours. For reducing the alignment error caused from incompletely available tooth contours, we propose pruning the outliers from each tooth contour after the first alignment then realigning the pruned contours. And for compensating the error when matching with the spatial feature of dental works due to imperfect tooth alignment, we propose using an additional frequency feature of DW, which is not affected by the tooth alignment. Meanwhile, for having more distinctive teeth available in a better quality image in general, we use bitewing radiographs instead of panoramic or periapical radiographs.

The remainder of this paper is organized as follows. In Section 2, we present a method of extracting effective tooth contours on which each point has an associated weight to facilitate shape matching of teeth. Then the algorithm of aligning two tooth contours based on the weighted Hausdorff distance is presented. In Section 3, a segmentation method of all dental works within an image and their contour representations in both spatial- and frequency-domains is presented. In Section 4, three metrics for teeth matching, dental work matching, and image matching are described. Experimental results, performance comparison in terms of retrieval accuracy, and discussions are provided in Section 5. Finally, concluding remarks are given in Section 6.

2. Alignment of effective tooth contours using weighted Hausdorff distance

Both teeth and dental works are used for identification in this paper. In teeth matching, the contour of each tooth in the query image is matched in spatial domain to the contour of each tooth in the database images; whereas in dental work matching, the contour of each dental work is matched in both spatial and frequency domains to each dental work in the database images. As each tooth and dental work must firstly be segmented from the images and the matching pair must be well aligned before matching, we describe teeth segmentation, contour extraction, and alignment of teeth in this section and those of dental works in the next section.

2.1. Segmentation of teeth

Both shapes and sizes of teeth provide important information for dental identification. As the scale, the orientation, and the translation of PM and AM radiographs are generally different due to view and age variations, each tooth must be segmented and the tooth pair to be matched must be well aligned to each other so that the pair can be matched fairly when using spatial features. Several good progresses for teeth segmentation had been made in the past few years [3,5,13,14]. In this paper, we use the segmentation method in Ref. [3], which was adapted from Ref. [5]. That is, we first enhance the image to separate gums from teeth. We then apply Canny edge detection [15] to the enhanced image to detect all edges and widen the edges by morphological dilation [16]. Next, we apply the iterative thresholding method using the average intensity of the edge pixels as an initial threshold to obtain a binary image with teeth in white and background in black. Using the binary image, we apply horizontal projection followed by vertical projection to separate it into regions of interest (ROIs) so that each one contains a tooth. Finally an edge operator is applied to each ROI followed by equal point sampling and B-spline fitting to obtain the contour of each tooth.

2.2. Contour extraction and alignment

After teeth segmentation, a connected component analysis [16] starting from the left-end point is applied to each tooth to

obtain a series of N connected contour points $Q_{Teeth}(n)=(x(n),y(n))$, $n=1,\ldots,N$. As mentioned in the previous Section 2.1, Q_{Teeth} must be well aligned to the database tooth contour D_{Teeth} so that a valid distance between the two can be computed. In this paper, we propose a contour alignment method based on the *weighted* Hausdorff distance, which is enhanced from a contour alignment method based on both affine transformation and Partial bi-directional Hausdorff distance (*HD*) [4].

The affine transform of a point in $Q_{Teeth}(n)$ is defined as [4]

$$T(\bullet)=\begin{pmatrix}\cos\theta & \sin\theta\\ -\sin\theta & \cos\theta\end{pmatrix}\begin{pmatrix}s_x & 0\\ 0 & s_y\end{pmatrix}+\begin{pmatrix}t_x\\ t_y\end{pmatrix} \tag{1}$$

where θ is the rotation angle; t_x and t_y are the translations along the x- and y-axis, respectively; s_x and s_y are the scaling factors in the horizontal and vertical directions, respectively.

Partial bi-directional Hausdorff distance between two sets of connected points **A** and **B**, which is a variant of bi-directional Hausdorff distance [17], is defined as follows [4]:

$$HD(\mathbf{A},\mathbf{B})=\max(h_K(\mathbf{A},\mathbf{B}),h_L(\mathbf{B},\mathbf{A})) \tag{2}$$

where

$$h_K(\mathbf{A},\mathbf{B})=K^{th}_{a\in\mathbf{A}}d(a,\mathbf{B})=K^{th}_{a\in\mathbf{A}}(\min_{b\in\mathbf{B}}d(a,b))=K^{th}_{a\in\mathbf{A}}(\min_{b\in\mathbf{B}}\|a-b\|) \tag{3}$$

$$h_L(\mathbf{B},\mathbf{A})=L^{th}_{b\in\mathbf{B}}d(b,\mathbf{A})=L^{th}_{b\in\mathbf{B}}(\min_{a\in\mathbf{A}}d(b,a))=L^{th}_{b\in\mathbf{B}}(\min_{a\in\mathbf{A}}\|b-a\|) \tag{4}$$

That is, $HD(\mathbf{A},\mathbf{B})$ is defined as the larger one of two distances: distance from set **A** to set **B** and distance from **B** to **A**. The distance from **A** to **B** is defined as the Kth largest distance between any point a in **A** and the set **B**, which is the shortest one among all distances between point a and each point in **B.** Similarly, the distance from **B** to **A** is defined as the Lth largest distance between any point b in **B** and the set **A**, which is the shortest one among all distances between point b and each point in **A**. Note that Kth (or Lth) is for determining how many points in set **A** (or **B**) can be discarded to obtain good results for an impulse noise case. For cases of Gaussian noise, $h_k(\mathbf{A},\mathbf{B})$ and $h_L(\mathbf{B},\mathbf{A})$can be replaced with the average of all distances from each point of a set to the other set as in Eqs. (5) and (6) [18].

$$h_{avg}(\mathbf{A},\mathbf{B})=\frac{1}{|\mathbf{A}|}\sum_{a\in\mathbf{A}}d(a,\mathbf{B}) \tag{5}$$

$$h_{avg}(\mathbf{B},\mathbf{A})=\frac{1}{|\mathbf{B}|}\sum_{b\in\mathbf{B}}d(b,\mathbf{A}) \tag{6}$$

where $|\mathbf{X}|$ denotes the cardinality of set **X**.

The contour alignment algorithm in [4] is briefly described as follows:

Algorithm. Contour alignment

Input: Two sequences of points Q_{Teeth} and D_{Teeth}.
Output: A sequence of points $T(Q_{Teeth})$ aligned to D_{Teeth}.

1. Select a set of different parameters (θ, s_x, s_y, t_x, t_y) and transform each point in Q_{Teeth} using Eq. (1) to obtain $T(Q_{Teeth})$.
2. Compute partial bi-directional Hausdorff distance between $T(Q_{Teeth})$ and D_{Teeth} using Eqs. (2)–(4).
3. Repeat steps 1 and 2 for all parameters in the trying range.
4. Return the transformed sequence $T(Q_{Teeth})$ that gives the minimum $HD(T(Q_{Teeth}),D_{Teeth})$.

The above alignment algorithm is not always satisfactory, because the segmented tooth contours of the PM–AM pair may not appear the same either in shape or in length or both due to poor image quality or view variation. To obtain a better alignment result, we propose two enhancements to the aforementioned contour alignment algorithm: weighted Hausdorff distance for shape difference and outlier detection and exclusion for length difference.

2.3. Contour alignment based on weighted Hausdorff distance of contour pair with outliers pruned

Our proposed Partial bi-directional weighted Hausdorff distance, abbreviated as weighted Hausdorff distance and denoted by *wHD* in this paper, can be calculated using Eqs. (2)–(4) but replacing $d(a,b)=\|a-b\|$ with $d^w(a,b)=(1/2)(W_a+W_b)\times\|a-b\|$, where W_a and W_b are the weights associated with points a and b, respectively. The weight of each contour point is calculated as follows.

2.3.1. Point weight calculation

The weight of a contour point is defined as its reliability of being a reliable contour point. We consider a contour point reliable when its local contrast is high and its neighborhood's intensity distribution is close to bimodal. The rationale can be better explained from the following two pairs of PM–AM images.

As shown in Fig. 2(a) and (b), which is a PM–AM image pair, the thickness and the shade of the crown part appear different due to view/illumination variation. Similarly, as shown in Fig. 3(a) and (b), the ways that two neighboring teeth appear overlapped (pointed by an arrow) are also different. Such differences lead to inconsistent teeth segmentation for the PM–AM contour pair (shown in red lines), and result in unsatisfactory alignment of the respective tooth pair using the contour alignment algorithm described in Section 2.2, as shown in Fig. 2(i) and Fig. 3(i), respectively. In other words, the contour points extracted from the crown part in Fig. 2 or from the teeth overlapped areas in Fig. 3 are not reliable and should be weighted less for better alignment. Notice that in the neighborhood of these unreliable contour points, either the intensity contrast is low or the histogram is not close to bimodal. Thus, we define the reliability of a contour point as the combination of contrast reliability and level-noise reliability, which are described as follows:

(i) **Contrast reliability**
We define the contrast reliability of a given point n in Q_{Teeth} as

$$R^C_{QTeeth}(n)=\sum_{u\in\mathbf{N}}(g(n)-g(u))^2 \tag{7}$$

where $g(u)$ is the gray value of point u belonging to the 11×11 neighborhood (N) of the given point n in Q_{Teeth}. That is, the bigger the contrast of the given point n, the more contrast-reliable the point is. Notice that we do not use entropy to calculate contrast reliability because it cannot reflect the degree of contrast's strength across the contour line of a tooth while Eq. (7) can.

(ii) **Level-noise reliability**
We define the level-noise reliability of a given point n as

$$R^N_{QTeeth}(n)=\begin{cases}(p-1)^{-1} & \text{if } p\geq 2\\ 0 & \text{otherwise}\end{cases} \tag{8}$$

where $p(>=0)$ is the number of histogram peaks of the 27×27 neighborhood of the given point n. A histogram peak is defined as the place where frequency differences of a particular gray level and its two immediate neighboring gray levels are at least 10 pixels. That is, the noisier the neighborhood of a given point is (or the more the number of histogram peaks), the less level-noise reliable the point is. In particular, a point is most level-noise reliable when the number of histogram peaks of the neighborhood is equal to 2, and is

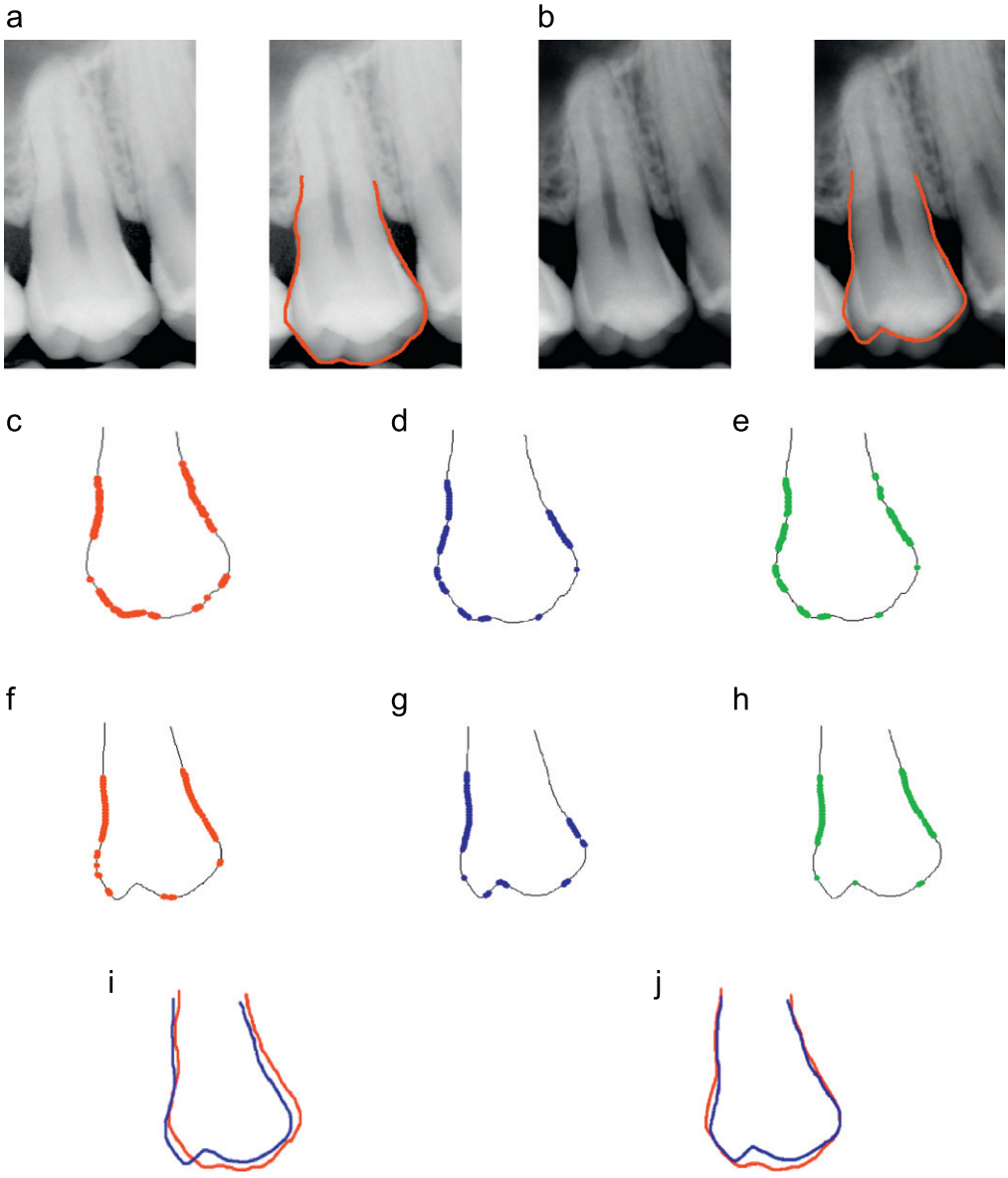

Fig. 2. Alignment of PM–AM tooth pair-1 where points with larger weight concentrate on side-contour. Alignment based on *wHD* has a better matching result than alignment based on traditional *HD*. (a) PM tooth and segmented contour; (b) AM tooth and segmented contour; PM: (c) Contour points with top-30% contrast-reliability; (d) Contour points with top-30% level-noise-reliability; (e) Contour points with top-30% combined weight; AM: (f) Contour points with top-30% contrast-reliability; (g) Contour points with top-30% level-noise-reliability; (h) Contour points with top-30% combined weight; (i) Alignment based on *HD*; (j) Alignment based on *wHD*. (For interpretation of the references to color in this figure legend, the reader is referred to the web version of this article.)

least level-noise reliable when the number of histogram peaks is less than 2. Note that the window size for computing level-noise reliability is bigger than that for computing contrast reliability, because we want to consider all different shades of crown part when computing such reliability. Note also that we do not use entropy to calculate level-noise reliability because Eq. (8) can reflect the number of various intensity levels within the 27×27 neighborhood of point n more directly.

Thus, the normalized weight of a point n in contour Q_{Teeth} can be obtained by

$$W_{QTeeth}(n) = \frac{1}{2}\left(\frac{R^C_{QTeeth}(n)}{\sum_{i=1}^{|QTeeth|} R^C_{QTeeth}(i)} + \frac{R^N_{QTeeth}(n)}{\sum_{i=1}^{|QTeeth|} R^N_{QTeeth}(i)}\right) \tag{9}$$

Similarly, the normalized weight of a point n in D_{Teeth} can be obtained by

$$W_{DTeeth}(n) = \frac{1}{2}\left(\frac{R^C_{DTeeth}(n)}{\sum_{i=1}^{|DTeeth|} R^C_{DTeeth}(i)} + \frac{R^N_{DTeeth}(n)}{\sum_{i=1}^{|DTeeth|} R^N_{DTeeth}(i)}\right) \tag{10}$$

In the above two equations, $|Q_{Teeth}|$ and $|D_{Teeth}|$ are the lengths of tooth contours Q_{Teeth} and D_{Teeth}, respectively.

We use two typical examples to demonstrate the rationale behind the design concept of reliability and weight of a contour point. Fig. 2(c)–(h) and Fig. 3(c)–(h) illustrate the points having top-30% contrast-reliability, level-noise-reliability, and combined weight of the PM tooth and the AM tooth, respectively. Notice that, in Fig. 2(e) and (h), majority of contour points having top-30% weight appear on the side-contour of a tooth, because they have both high contrast and noise-level reliabilities. Only few points having top-30% weight appear in the crown-contour,

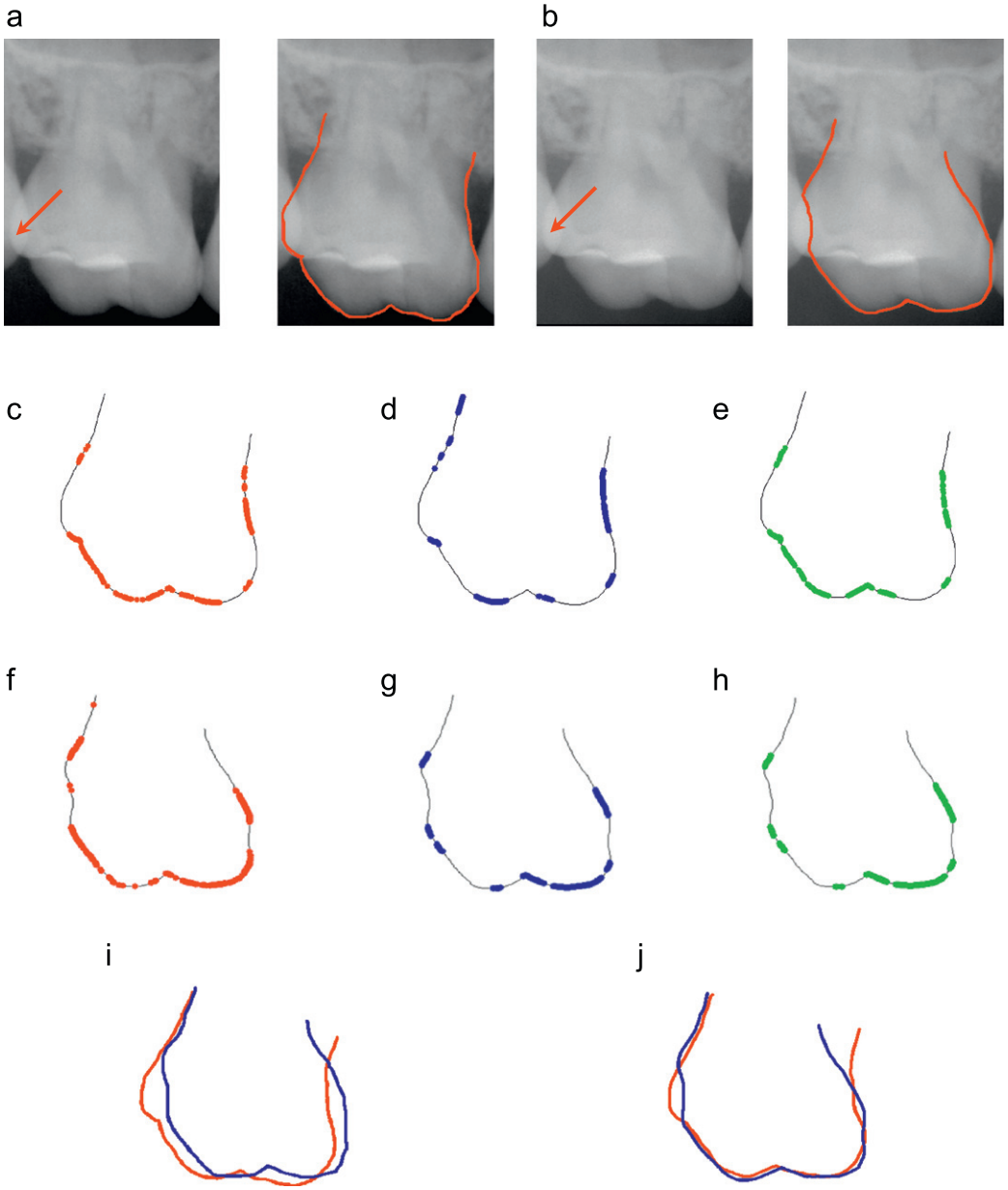

Fig. 3. Alignment of PM–AM tooth pair-2 where points with larger weight concentrate on crown-contour. Alignment based on *wHD* has a better matching result than alignment based on traditional *HD*. (a) PM tooth and segmented contour; (b) AM tooth & segmented contour; PM: (c) Contour points with top-30% contrast-reliability; (d) Contour points with top-30% level-noise-reliability; (e) Contour points with top-30% combined weight; AM: (f) Contour points with top-30% contrast-reliability; (g) Contour points with top-30% level-noise-reliability; (h) Contour points with top-30% combined weight; (i) Alignment based on *HD*; (j) Alignment based on *wHD*. (For interpretation of the references to color in this figure legend, the reader is referred to the web version of this article.)

because most of the crown-contour points have low level-noise reliability. Such a result reflects the fact that the crown-contour difference of the PM–AM tooth pair is large while the side-contour difference is small, as shown in Fig. 2(a) and (b). Thus, the side points should be weighted more than the crown points in order to obtain a better matching. On the contrary, more than half of the crown-contour points have top-30% weight in Fig. 3(e) and (h), because they have either high contrast reliability or high level-noise reliability or both. Only a few points with top-30% weight appear on the side-contour as shown in Fig. 3(h), because most of the side-contour points are either within the gum or overlapped with the neighboring tooth and hence have low contrast-liability and low level-noise reliability. Again, such a result also correctly reflects the fact that the side-contours of the respective PM and AM tooth do not match very well with each other, as shown in Fig. 3(a) and (b), and thus should be assigned with less weight to achieve a better alignment. Fig. 2(j) and Fig. 3(j) show the respective alignment result of both PM–AM tooth pairs based on the proposed weighted *HD*, where both PM tooth contours (red) coincide with the AM contours (blue) much better than the alignment results based on the traditional *HD* as shown in Fig. 2(i) and Fig. 3(i), respectively. The above two examples demonstrate the usefulness of contrast-reliability, level-noise reliability, and consequently the weights of contour points.

2.3.2. *Contour outlier detection and pruning*

Outliers are generally defined as patterns in a dataset that do not conform to a well defined notion of normal behavior [19]. However, in shape registration such as tooth contour alignment, outliers are regarded as points, which have no corresponding points in the

counterpart curve for matching. Chen and Jain [10] proposed a shape registration algorithm that finds a corresponding point in the AM contour point set called *BP* for each of the transformed PM contour point set called *TAP*, then selects the one with the shortest distance as the final corresponding point when more than one *TAP* point corresponds to the same *BP* point. Those points without corresponding points are considered as outliers and the subset of *TAP* with outliers removed is the new transformed PM contour-point set called *TAP′*. Their shape registration algorithm can achieve tooth contour matching in a systematic way.

Instead of using shape registration algorithm to remove outliers, we use a heuristic outlier-removing method to incorporate with our investigation that a large percentage of outliers appear in the terminal parts of a tooth contour, because the terminal parts are embedded in the gum and therefore look fuzzier and more uncertain in dental radiographs. Observing Fig. 4(a), which is a non-fully overlapped transformed PM and AM contour pair, we notice that the non-overlapped segments as shown in segments R_1 and R_2 occur at either or both sides of the transformed PM contour (denoted $T(Q_{Teeth})$ in follows) or the AM contour (denoted D_{Teeth} in follows). It is reasonable to say that points on the segments R_1 of $T(Q_{Teeth})$ and R_2 of D_{Teeth} have no corresponding point for matching and can be regarded as outliers of this contour pair. Notice that the y-coordinate of all points in R_1 and R_2 falls in the range of $[\min\{T(Q_{Teeth}(0))_y, D_{Teeth}(0)_y\}, \max\{T(Q_{Teeth}(0))_y, D_{Teeth}(0)_y\}]$ and $[\min\{T(Q_{Teeth}(N-1))_y, D_{Teeth}(N-1)_y\}, \max\{T(Q_{Teeth}(N-1))_y, D_{Teeth}(N-1)_y\}]$, respectively, if we number the N points from 0 to $N-1$ on each of two contours from the left-end to the right-end. Thus, for contour pair $T(Q_{Teeth})$ and D_{Teeth}, we define outliers as those points with their y-coordinates falling in the range of $[\min\{T(Q_{Teeth}(0))_y, D_{Teeth}(0)_y\}, \max\{T(Q_{Teeth}(0))_y, D_{Teeth}(0)_y\}]$ and $[\min\{T(Q_{Teeth}(N-1))_y, D_{Teeth}(N-1)_y\}, \max\{T(Q_{Teeth}(N-1))_y, D_{Teeth}(N-1)_y\}]$, as shown in green circles in Fig. 4(b).

2.3.3. Proposed contour alignment algorithm

Algorithm. Effective contour alignment based on weighted Hausdorff distance

Input: Two contours Q_{Teeth} and D_{Teeth}.
Output: Two pruned and well aligned contours $T(\tilde{Q}_{Teeth})$ and $\tilde{D}_{Teeth}$ ready for matching.

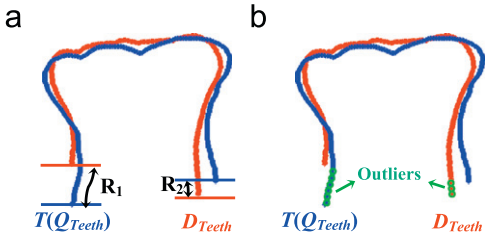

Fig. 4. Illustration of outliers of a transformed query tooth $T(Q_{Teeth})$ and database tooth D_{Teeth} contour pair. (a) Non-fully overlapped $T(Q_{Teeth})$ and D_{Teeth}; (b) Detected outliers. (For interpretation of the references to color in this figure legend, the reader is referred to the web version of this article.)

1. Calculate the normalized weights W_{QTeeth} and W_{DTeeth} for each point on the contours Q_{Teeth} and D_{Teeth}.
2. Perform contour alignment as described in Section 2.2 for Q_{Teeth} and D_{Teeth} using *weighted* distance $d^w(a,b)=(1/2)[W_{Qteeth}(a)+W_{Dteeth}(b)]\|a-b\|$ between point a in Q_{Teeth} and point b in D_{Teeth} and obtain an aligned contour $T(Q_{Teeth})$.
3. Resample each of contours $T(Q_{Teeth})$ and D_{Teeth} evenly from the left-end to the right-end to obtain two sequences of N points $T(Q_{Teeth}(i))$ and $D_{Teeth}(i)$, $i=0,\ldots,N-1$.
4. Trace the contour points $T(Q_{Teeth}(i))$ and $D_{Teeth}(i)$ from $i=0$ to $N-1$. The points with their y-coordinates falling in the range $[\min\{T(Q_{Teeth}(0))_y, D_{Teeth}(0)_y\}, \max\{T(Q_{Teeth}(0))_y, D_{Teeth}(0)_y\}]$ and $[\min\{T(Q_{Teeth}(N-1))_y, D_{Teeth}(N-1)_y\}, \max\{T(Q_{Teeth}(N-1))_y, D_{Teeth}(N-1)_y\}]$ are regarded as outliers.
5. Remove all the outlier points from $T(Q_{Teeth})$ and D_{Teeth} to obtain two pruned contours $\tilde{Q}_{Teeth}$ and $\tilde{D}_{Teeth}$ and re-calculate the normalized weights $\tilde{W}_{QTeeth}$ and $\tilde{W}_{DTeeth}$ for each point on the pruned contours $\tilde{Q}_{Teeth}$ and $\tilde{D}_{Teeth}$.
6. Align $\tilde{Q}_{Teeth}$ to $\tilde{D}_{Teeth}$ to obtain the final result $T(\tilde{Q}_{Teeth})$ using the contour alignment algorithm as described in Section 2.2 and *weighted* distance $d^w(a,b)=(1/2)[\tilde{W}_{QTeeth}(a)+\tilde{W}_{DTeeth}(b)]\|a-b\|$ between point a in $\tilde{Q}_{Teeth}$ and point b in $\tilde{D}_{Teeth}$.
7. Return $T(\tilde{Q}_{Teeth})$ and $\tilde{D}_{Teeth}$.

Fig. 5(d) is the alignment result using *wHD* of the contours in Fig. 5(a) and (b), which is significantly better than the alignment result using HD of both contours, as shown in Fig. 5(c). Fig. 5(e) is the alignment result using the proposed effective (or pruned) contour alignment method, which is even better than the result shown in Fig. 5(d).

3. Dental work extraction and representation

Like teeth matching, the contours of dental works are also used for dental work matching. But, instead of only matching the contour of dental works in spatial domain as in teeth matching, we also match the contour of dental works in frequency domain so that spatial information such as shape, size, location, and orientation will all be considered while the differences caused from imperfect teeth alignment and boundary disturbances can be tolerated.

3.1. Segmentation of dental works

We segment an entire image to obtain all the dental works within it. However, dental radiographs often have uneven illumination problem that causes non-DWs such as enamels to appear as bright as or even brighter than DWs. Thus, using a single threshold to segment the entire image without preprocessing is inappropriate and would often mistake some non-DWs as DWs. Instead of directly thresholding the entire image to get the coarse shapes of DWs in the first stage as in [11], we preprocess the image to reduce most irrelevant information and then threshold

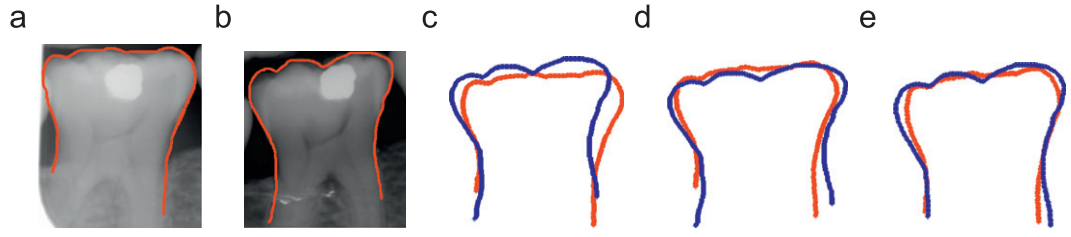

Fig. 5. A comparison of regular contour alignment and the proposed effective contour alignment. (a) The query tooth. (b) The database tooth. (c) Alignment based on *HD* of the original contours (regular contour alignment). (d) Alignment based on *wHD* of the original contours. (e) Alignment based on *wHD* of the effective (or pruned) contours.

the remaining pixels to get the coarse shapes of DWs. We then obtain the complete shape of each DW by region growing instead of using a separate snake as in [11]. Our dental work extraction procedure is detailed in the following:

1. Detect edge pixels by Canny filter. We apply Canny edge filter [15] to obtain the DW edge pixels around DWs and refine the edges by replacing each edge pixel with the brightest one in its 5×5 neighborhood.
2. Remove non-DW edges by intensity thresholding. We take the intensity histogram of the resulted edge pixels and smooth it with moving average filter. We then filter out those edge pixels with their intensity lower than the right-most-valley value of the histogram.
3. Remove non-DW edges by contour-length thresholding. We connect all edge pixels to segments and filter out those with length less than a preset threshold. At this time, the extracted contours may not be all complete, as shown inside the circles in Fig. 6(d)–(f), where (a)–(c) are the original images.
4. Obtain the complete shapes of DWs by region growing from the coarse contours. We use the center point of each contour as the seed of each DW region and iteratively merge in the 8-neighhood pixels of each pixel whose intensities are within $\pm \delta_I$ of the average intensity of the region and whose positions are within $\pm \delta_P$ of the minimum bounded region of the initial contour, where δ_I and δ_P are set by trial and error, until the region is no longer changed [20].

Fig. 6(g)–(i) are the well grown DWs after Step 4, which are indeed very close to the true DW shapes. Comparing to Fig. 6(j)–(l), which are the coarse shapes of the DWs extracted by the method in Ref. [11], our method indeed performs much better for handling uneven illuminated images.

3.2. Contour extraction and alignment of dental works

Similar to teeth matching, a connected component analysis [16] starting from the left or the right bottom point is applied to each DW to obtain a series of N connected contour points $z(n)=(x(n),y(n))$, $n=0,\ldots,N-1$.

When matching the DW contours in spatial domain, the contours under matching must be aligned first like teeth matching. However, two DWs with very similar shape may have different orientation/position relative to the tooth in which it resides. As shown inside the circles of Fig. 7(a)–(c), the DW in (a) (i.e., the query DW) is identical to (b) (i.e., the genuine DW) in both shape and position, but is only identical to (c) (i.e., the imposter DW) in shape. If we directly align the DW in (a) to the DW in (c), the difference of position relative to the tooth between these two DWs will be neglected. Thus, to preserve spatial

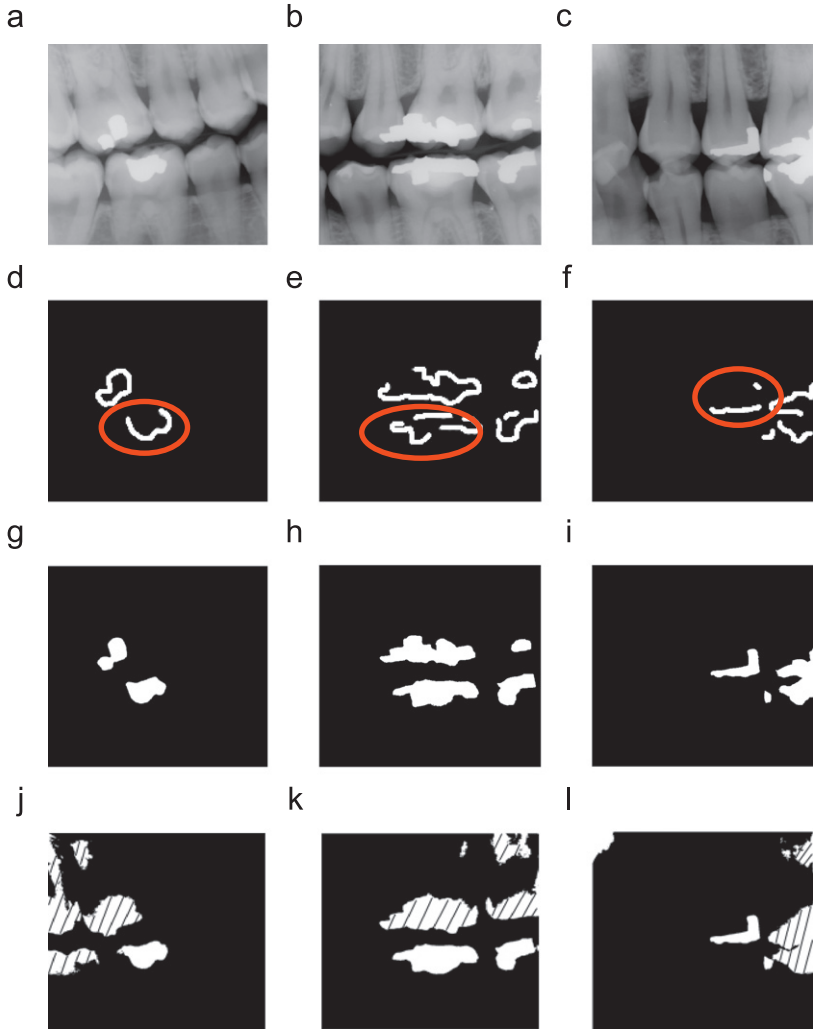

Fig. 6. Detected dental works (DWs) using our method and the method in Ref. [11]. (a)–(c) Original radiographs. (d)–(f) The coarse contours of DWs extracted by our method. (g)–(i) Complete shapes of the extracted DWs by our method. (j)–(l) The coarse shapes of DWs extracted by the method in Ref. [11].

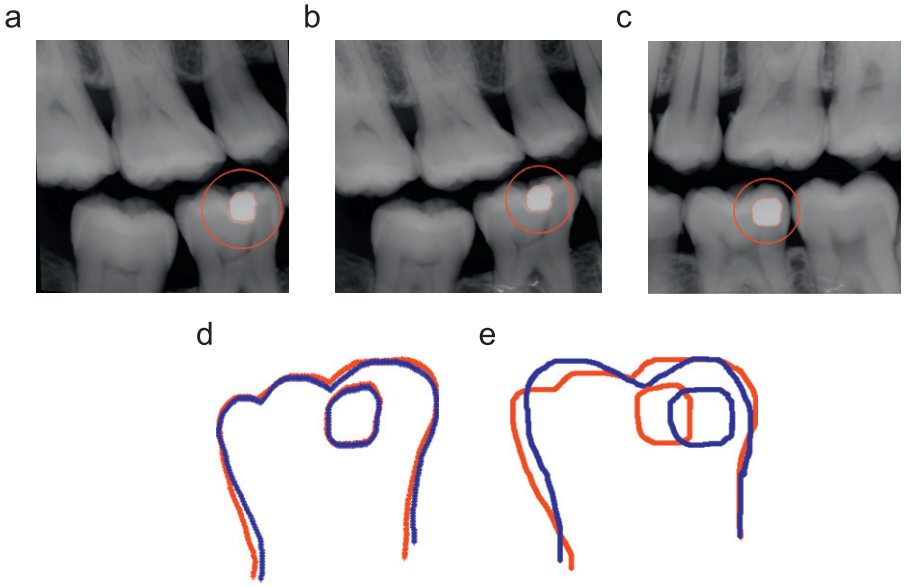

Fig. 7. The results of teeth alignment and dental work alignment with the parameters used in teeth alignment. (a) Query DW. (b) Genuine DW. (c) Imposter DW. (d) The contours of the DW in (b) and the DW in (a) being affine transformed with the teeth alignment parameters between (a) and (b). (e) The contours of the DW in (c) and the DW in (a) being affine transformed with the teeth alignment parameters between (a) and (c).

relationship between a DW and the tooth in which it resides, we simply affine transform the query DW using the optimum parameters obtained from teeth alignment so that two DWs under matching will be well aligned and the difference of the position relative to the tooth between the DWs is also preserved. Fig. 7(d) shows the contours of the DW in (b) and the DW in (a) being affine transformed with the teeth alignment parameters between (a) and (b). Similarly, Fig. 7(e) shows the contours of the DW in (c) and the DW in (a) being affine transformed with the teeth alignment parameters between (a) and (c). Notice that the query DW is well overlapped with the genuine DW as shown in (d) and is partially overlapped with the imposter DW as shown in (e).

However, when the alignment on tooth contours is not good enough, the query DW may not be overlapped to the genuine DW as well as to the imposter DW, when the imposter DW happens to be similar to the genuine DW in both shape and position. Fig. 8(a)–(e) gives such an example, where (a) is the tooth containing the query DW, (b) is the tooth containing the genuine DW, (c) is the tooth containing an imposter DW, (d) is the contours of the DWs in (b) and (a) after teeth alignment, and (e) is the contours of the DWs in (c) and (a) after teeth alignment. Notice that the difference of two DWs in (d) appears bigger than that in (e) and will lead to incorrect matching if spatial feature such as Hausdorff distance or XOR method in [10] is used. To reduce matching errors resulted from unsatisfactory teeth alignment, we propose using an additional affine-transform invariant feature as follows.

3.3. Frequency domain feature of dental works

Adapting from [21] that used a set of normalized Fourier descriptors (NFDs) as the affine transformation invariant feature of tooth contour, we used a set of NFDs as the affine transformation invariant feature of DWs so that the difference of DWs under matching will not be affected by the result of teeth alignment.

The normalized Fourier descriptors of a dental work contour can be obtained by converting the coordinates of the dental work contour points to a series of N complex numbers $f(n)=x(n)+jy(n)$, $n=0,\ldots,N-1$, then taking the Fourier transform of the series $f(n)$ as

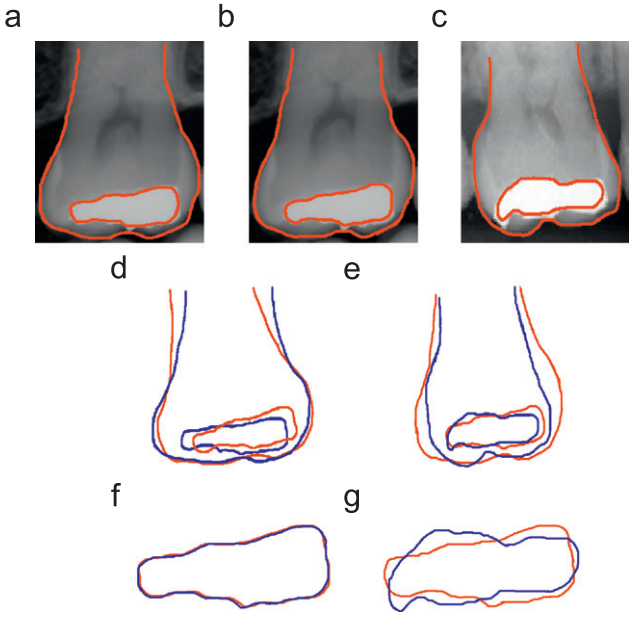

Fig. 8. The differences of two DW contours in spatial- and frequency domains. (a) Query DW. (b) Genuine DW. (c) Imposter DW. (d) The difference between two DW contours in (b) and (a) after teeth alignment. (e) The difference between two DW contours in (c) and (a) after teeth alignment. (f) The difference between two contours reconstructed from 50% of the Fourier descriptors of DWs in (a) and (b). (g) The difference between two contours reconstructed from 50% of the Fourier descriptors of DWs in (a) and (c).

$$F(u)=DFT(f(n))=\frac{1}{N}\sum_{n=0}^{N-1}f(n)e^{-j(2\pi nu/N)} \tag{11}$$

$u=0,1,\ldots,N-1$. The series of Fourier coefficients is then normalized as

$$DW_F=\left[\frac{|F(2)|}{|F(1)|},\frac{|F(3)|}{|F(1)|},\ldots,\frac{|F(N-1)|}{|F(1)|}\right] \tag{12}$$

Notice that discarding the first coefficient $F(0)$ is to achieve translation invariance; dividing all other coefficients by the second coefficient $F(1)$ is to achieve scale invariance; and taking the magnitude of the coefficients is for rotation invariance [21]. Fig. 8(f) and (g) shows the respective shape contours reconstructed from 50% DW_F of the DWs in Fig. 8(a) and (b), and in Fig. 8(a) and (c). Notice that the contour difference in Fig. 8(f) is almost negligible while the difference in Fig. 8(g) becomes obvious. In other words, the spatial contour difference caused from unsatisfactory teeth alignment as shown in Fig. 8(d) no longer exists in Fig. 8(f).

4. Dental identification

Teeth matching, dental work matching, and image matching are performed for dental identification. The matching is performed by measuring the distances between the query object (tooth, dental work, or image) and each of the database objects to generate a matching list. The list is then ranked in an ascending order. The accurate top-K retrieval of a given query object means that the corresponding genuine database object is ranked the Kth in the matching list and top-K retrievals means that the corresponding genuine database object is ranked less than or equal to the Kth in the matching list. Thus, the retrieval accuracy using top-K(%) retrievals is calculated by the total number of accurate genuine objects ranked less than or equal to the Kth in the matching list divided by the total number of objects (teeth, dental works, or images) in the database. Three metrics for teeth matching, dental work matching, and image matching are proposed as follows.

4.1. Metric for teeth matching

Assume that a tooth contour Q_{Teeth} has been aligned to another tooth contour D_{Teeth} using the effective contour alignment algorithm presented in Section 2.3. Note that both Q_{Teeth} and D_{Teeth} are effective contours (i.e., contours with outliers being pruned). Now we propose a metric for teeth matching based on *weighted* Hausdorff distance, denoted as d_{Teeth}^{wHD}, to measure the distance between the query contour Q_{Teeth} and the database contour D_{Teeth} as follows:

$$d_{Teeth}^{wHD}(Q_{Teeth},D_{Teeth}) = \max(h^w(D_{Teeth},Q_{Teeth}),h^w(Q_{Teeth},D_{Teeth})) \tag{13}$$

$$h^w(Q_{Teeth},D_{Teeth}) = \frac{1}{N_a}\sum_{a\in Q_{Teeth}}\frac{1}{2}(W_{QTeeth}(a)+W_{DTeeth}(Cor(a)))d(a,(Cor(a))) \tag{14}$$

$$h^w(D_{Teeth},Q_{Teeth}) = \frac{1}{N_b}\sum_{b\in D_{Teeth}}\frac{1}{2}(W_{DTeeth}(b)+W_{QTeeth}(Cor(b)))d(b,(Cor(b))) \tag{15}$$

where $W_{QTeeth}(a)$ and $W_{DTeeth}(b)$ are the normalized weights of points a in Q_{Teeth} and b in D_{Teeth}, respectively; $Cor(k)$ is a point in D_{Teeth}/Q_{Teeth} corresponding to point k in Q_{Teeth}/D_{Teeth} with $d(k, Cor(k))$ being the minimum distance of point k to the contour D_{Teeth}/Q_{Teeth}; $W_{DTeeth}(Cor(a))$ and $W_{QTeeth}(Cor(b))$ are the weights of the points $Cor(a)$ in D_{Teeth} and $Cor(b)$ in Q_{Teeth}, respectively. According to our observation, we found that discarding the largest 20% point distances from each contour will allow us to reduce the effect of noises resulted from poor image quality. Therefore, we set $N_a=0.8q$ and $N_b=0.8p$, where q and p are the number of points in Q_{Teeth} and of D_{Teeth}, respectively.

4.2. Metric for dental work matching

The metric for dental work matching between a query dental work Q_{DW} and a database dental work D_{DW} is based on a combination of the following two measures: (1) average Hausdorff distance between the contour point sequences of the query DW (denoted as Q_{DW}^S) and database DW (denoted as D_{DW}^S), and (2) the root mean square error between the normalized Fourier descriptors of the query DW (denoted as Q_{DW}^F) and database DW (denoted as D_{DW}^F). Note that we use the average Hausdorff distance instead of weighted Hausdorff distance as the metric for matching dental works in spatial domain, because the contours of DWs are mostly sharp and the intensity histograms of their neighborhood are mostly close to bimodal.

The average Hausdorff distance is defined as

$$d_{DW}^{avgHD}(T(Q_{DW}^S),D_{DW}^S) = \max(h_{avg}(D_{DW}^S,T(Q_{DW}^S)),h_{avg}(T(Q_{DW}^S),D_{DW}^S)) \tag{16}$$

where $h_{avg}(D_{DW}^S,T(Q_{DW}^S))$ and $h_{avg}(T(Q_{DW}^S),D_{DW}^S)$ can be calculated using Eqs. (5) and (6). Notice that, in Eq. (16), Q_{DW}^S is firstly affine transformed to $T(Q_{DW}^S)$ using the optimum parameters obtained from the teeth alignment before being matched to D_{DW}^S. Notice also that contours of DWs are not pruned because they are both closed contours. Thus, d_{DW}^{avgHD} not only measures the difference of the shapes between the pair of two DWs under matching, but also the difference of the positional distance between the two.

The metric in frequency domain is used to measure the matching distance between two sequences of normalized Fourier descriptors (NFDs). Since NFDs are affine-transform invariant, and hence no alignment between the two sequences are required. This metric can be computed as the root mean square error (RMSE) of the two sequences of NFDs using the following equation:

$$d_{DW}^{FD}(Q_{DW}^F,D_{DW}^F) = \sqrt{\frac{1}{N}\sum_{k=1}^{N}|Q_{DW}^{Fk}-D_{DW}^{Fk}|^2} \tag{17}$$

where Q_{DW}^{Fk} and D_{DW}^{Fk} are the respective kth NFD of the query sequence and the database sequence obtained from Eq. (12), and N is the total number of NFDs used for each sequence. In general, the first few coefficients (e.g. the top 10–20%) of the descriptors are enough for differentiating two obviously different shapes [16]. However, many DWs are not significantly different in shape and can only be differentiated by considering more detailed information. Thus, we propose using the first 50% of NFDs so that they are not only enough to differentiate the shape difference but also insensitive to boundary noises.

As mentioned earlier, using spatial-domain metric d_{DW}^{avgHD} cannot handle imperfect alignment situation but frequency-domain metric d_{DW}^{FD} can, because NFDs are affine-transform invariant. On the other hand, using affine-transform invariant metric d_{DW}^{FD} may retrieve dental works of similar shape with different position or orientation, but using spatial metric d_{DW}^{avgHD} will not have this problem because it considers all spatial relationships. To compensate each other's drawback while taking the advantage of each individual, the average of both normalized frequency- and spatial-domain metrics is used and defined as follows:

$$d_{DW}^{HF}(Q_{DW},D_{DW}) = \frac{(Nom(d_{DW}^{avgHD})+Nom(d_{DW}^{FD}))}{2} \tag{18}$$

where

$$Nom(x) = \frac{1}{1+\exp(-Z_x)}$$

$$Z_x = \frac{x-\mu_x}{\sigma_x}$$

$$\mu_x = \frac{1}{|\mathbf{A}_x|}\sum_{\forall b \in \mathbf{A}_x} b, \quad \sigma_x = \sqrt{\frac{1}{|\mathbf{A}_x|-1}\sum_{\forall b \in \mathbf{A}_x}(b-\mu_x)^2} \tag{19}$$

That is, Z_x is the Z-score of a matching distance x and $Nom(x)$ is Z_x being normalized to be within [0,1]. Note that data falling at the right side of two times of standard deviation are neglected when computing μ and σ.

4.3. Metric for image matching

The similarity between the query PM image Q_{Image} and each AM image D_{Image} in the database is measured by averaging the matching distances of (1) all teeth only and (2) all teeth and dental works in the query image, respectively.

4.3.1. Identification by teeth

The metric d^{Teeth}_{Image}, which only measures the distance between tooth contours, is calculated by

$$d^{Teeth}_{Image}(Q_{Image}, D_{Image}) = \frac{1}{Nq}\sum_{i=1}^{Nq}\min_{j=1\ldots Nd}\{Nom(d^{wHD}_{Teeth_{ij}})\} \tag{20}$$

where $d^{wHD}_{Teeth_{ij}}$ represents the matching distance between the ith tooth in the query image and the jth tooth in the database image; Nq and Nd are the number of teeth in the query image and the database image, respectively. In other words, for each tooth in the query image, the minimum matching distance among all teeth in the database image is firstly identified. All the minimum matching distances in the query image are then averaged as the matching distance of the query image.

4.3.2. Identification by teeth and dental works

The distance $d^{Teeth\&DW}_{Image}$ is calculated by combining both the matching distances of teeth $d^{wHD}_{Teeth_{ij}}$ in Eq. (13) and the matching distances of dental works $d^{HF}_{DW_{ij}}$ in Eq. (18) as follows:

$$d^{Teeth\&DW}_{Image}(Q_{Image}, D_{Image}) = \frac{1}{Nq}\sum_{i=1}^{Nq}\min_{j=1\ldots Nd}((1-w)Nom(d^{wHD}_{Teeth_{ij}}) + wNom(d^{HF}_{DW_{ij}})) \tag{21}$$

$$w = \begin{cases} \frac{N_T}{N_D+N_T} & \text{if the query tooth contains DW} \\ 0 & \text{otherwise} \end{cases} \tag{22}$$

N_T and N_D are the respective number of teeth and dental works in the database. Note that w is fixed for every tooth and is greater than 1/2 when the query tooth has dental work, because the number of dental works in the database will never be greater than the number of teeth in the database (i.e., $N_T > N_D$). In other words, we choose to weigh the dental work more than the tooth within which it resides, since the dental work is not as sensitive to view and age variations as the tooth contour.

5. Experimental results and comparisons

We used 93 database images (containing a total of 552 teeth and 122 dental works) and 35 query images (containing a total of 220 teeth and 38 dental works) to evaluate the performance of teeth matching, dental work matching, and image matching. Among the 35 query images, 12 images were obtained from our team members and the rest of 23 images were obtained from various websites. Among the 93 database images, 12 images were also obtained from our team members at the time about 3-month earlier than their corresponding images were taken. Additional 23 database images were created by resizing in X and/or Y directions, rotating, and adjusting the illumination of their corresponding query images. The rest of 58 database images were collected from various websites and used as hoax identities. Although our database is not completely real, the way of constructing such an emulated database for experiment is quite reasonable and close to real to a certain degree. Fig. 9 shows some query images (treated as PM) and database images (treated as AM) used in our experiments. In order to reduce the search space of matching, each tooth or dental work is only matched against the tooth or dental work in the same jaw. Table 1 lists the composition of teeth and dental works in the database for experiments.

5.1. Performance of teeth matching

We compare the effectiveness of three teeth matching methods that respectively use (1) partial bi-directional Hausdorff distance (*HD*) of the original contour, (2) partial bi-directional *weighted* Hausdorff distance (*wHD*) of the original contour, and (3) *wHD* of the effective contour (i.e., pruned contour) of each PM query tooth against all AM tooth contours in the database. Table 2 shows the retrieval accuracy of all three methods. Among all queries of teeth, the accuracy of Method-(1), -(2), and -(3) are 38.2%, 40.9%, and 43.5%, respectively, for the upper jaw and 36.2%, 37.1%, and 47.6%, respectively for the lower jaw using the top-1

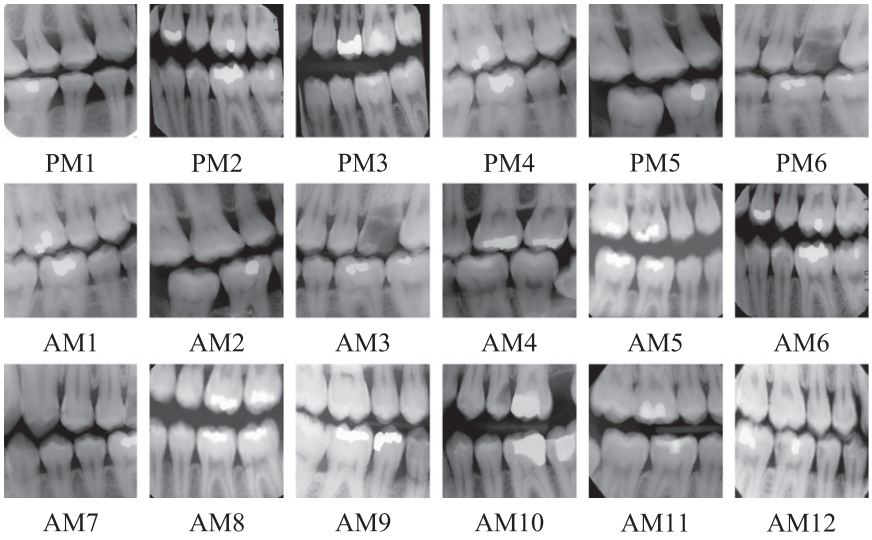

Fig. 9. Some query images (treated as PM) and database images (treated as AM) used in the experiments.

Table 1
The composition of experimental database.

Teeth	# of images	# of teeth	
		Upper jaw	Lower jaw
PM	35	115	105
AM	93	285	267
Dental Works	# of images	# of dental works	
		Upper jaw	Lower jaw
PM	17	18	20
AM	51	52	70

Table 2
The comparison on teeth retrieval accuracy.

	Jaw	Top-*N* retrievals					
		N=1	*N*=3	*N*=5	*N*=10	*N*=15	*N*=20
(1)	upper	44/115	60/115	65/115	79/115	83/115	85/115
		38.2%	52.2%	56.5%	68.7%	72.2%	73.9%
	lower	38/105	52/105	66/105	78/105	85/105	90/105
		36.2%	49.5%	62.9%	74.3%	80.9%	85.7%
(2)	upper	47/115	77/115	87/115	95/115	98/115	98/115
		40.9%	66.9%	75.7%	82.6%	85.2%	85.2%
	lower	39/105	60/105	69/105	79/105	88/105	91/105
		37.1%	57.1%	65.7%	75.2%	83.8%	86.7%
(3)	upper	50/115	77/115	88/115	98/115	101/115	104/115
		43.5%	66.9%	76.5%	85.2%	87.8%	90.4%
	lower	50/105	72/105	83/105	91/105	91/105	94/105
		47.6%	68.6%	79.0%	86.7%	86.7%	89.5%

Method-(1): using metric d_{Teeth}^{HD} of original tooth contours.
Method-(2): using metric d_{Teeth}^{wHD} of original tooth contours.
Method-(3): using metric d_{Teeth}^{wHD} of effective tooth contours.

retrieval. Using top-5 retrievals, the accuracies of all three methods are raised to 56.5% (62.9%), 75.7% (65.7%), and 76.5% (79.0%), respectively, for the upper (lower) jaw. The retrieval accuracy of Method-(3) achieves 85% and above for both jaws when using top-10 retrievals, whereas the other two methods can only achieve this accuracy when using more than top-15 retrievals. In other words, when using top-5 retrievals, matching with *wHD* of the original contour (i.e., Method-(2)) can indeed improve the accuracy 19.2% (2.8%) for the upper (lower) jaw; and matching with *wHD* of the effective contours (i.e., Method-(3)) can further improve the accuracy 0.8% (13.3%) for the upper (lower) jaws. The improvements continue for top-10, -15, and -20 retrievals. Thus, Table 2 indicates that Method-(3) is superior to Method-(2), which in turn is superior to Method-(1).

5.2. Performance of dental works matching

We conducted dental works matching using the frequency-, spatial-, and combined-domain metrics (Method-(a), -(b), -(c)), respectively. Table 3 shows the comparison of retrieval accuracy on dental works matching. Among all queries of dental works, the retrieval accuracies of Methods-(a), -(b), and -(c) are 77.8%, 83.3%, and 94.4%, respectively, for the upper jaw and 65.0%, 65.0%, and 70.0%, respectively, for the lower jaw using the top-1 retrieval. Using top-3 retrievals, the accuracies of all three methods are raised to 83.3%, 94.4%, and 100% for the upper jaw and 90.0%, 80.0%, and 85.0%, respectively, for the lower jaw. It seems that there is no definite superiority between Method-(a) and Method-(b); however, when we combine Method-(a) and Method-(b) to form Method-(c), we found that Method-(c) outperforms Methods-(a) and -(b),

Table 3
The comparison on dental works retrieval accuracy.

	Jaw	Top-*N* retrievals				
		N=1	*N*=3	*N*=5	*N*=7	*N*=10
(a)	upper	14/18	15/18	17/18	18/18	18/18
		77.8%	83.3%	94.4%	100%	100%
	lower	13/20	18/20	18/20	18/20	19/20
		65%	90%	90%	90%	95%
(b)	upper	15/18	17/18	17/18	17/18	17/18
		83.3%	94.4%	94.4%	94.4%	94.4%
	lower	13/20	16/20	17/20	17/20	17/20
		65%	80%	85%	85%	85%
(c)	upper	17/18	18/18	18/18	18/18	18/18
		94.4%	100%	100%	100%	100%
	lower	14/20	17/20	17/20	19/20	19/20
		70%	85%	85%	95%	95%

Method-(a): using metric d_{DW}^{FD} of DW contours.
Method-(b): using metric d_{DW}^{avgHD} of DW contours.
Method-(c): using metrics $d_{DW}^{avgHD}+d_{DW}^{FD}$ of DW contours.

Table 4
The comparison on the accuracy of image matching.

	Jaw	Top-*N* retrievals				
		N=1	*N*=2	*N*=3	*N*=5	*N*=10
(A)	upper	17/35	20/35	24/35	29/35	31/35
		48.6%	57.1%	68.6%	77.1%	88.6%
	lower	20/35	22/35	24/35	25/35	29/35
		57.1%	62.9%	68.6%	71.4%	82.9%
	both	24/35	26/35	27/35	30/35	32/35
		68.6%	74.3%	77.1%	85.7%	91.4%
(B)	upper	26/35	31/35	32/35	34/35	34/35
		76.3%	88.6%	91.4%	97.1%	97.1%
	lower	26/35	29/35	30/35	33/35	34/35
		74.3%	82.9%	85.7%	94.3%	97.1%
	both	33/35	34/35	34/35	35/35	35/35
		94.3%	97.1%	97.1%	100%	100%
(C)	upper	27/35	32/35	33/35	35/35	35/35
		77.1%	91.4%	94.3%	100%	100%
	lower	29/35	32/35	33/35	34/35	34/35
		82.9%	91.4%	94.3%	97.1%	97.1%
	both	33/35	35/35	35/35	35/35	35/35
		94.3%	100%	100%	100%	100%

Method-(A): using metric d_{Teeth}^{HD} of the original tooth contours.
Method-(B): using metric d_{Teeth}^{wHD} of the effective tooth contours.
Method-(C): using metric d_{Teeth}^{wHD} of the effective tooth contours.
and metrics $(d_{DW}^{avgHD}+d_{DW}^{FD})$ of the DW contours.

respectively. Method-(a) will mistakenly match DWs, which are similar in shape and different in orientation/position, but Method-(b) will not; whereas Method-(b) could possibly mistakenly match an imposter DW instead of the genuine DW when imperfect alignment occurs, but Method-(a) will not make such mistakes as it does not require alignment. Thus, using combined metrics can indeed compensate each other's drawback and improve the retrieval accuracy, as demonstrated in Table 3.

5.3. Performance of image matching

To evaluate the performance of image matching, 35 query PM images were used to match with 93 database AM images by the following methods: (A) teeth-matching based on *HD* for the original contours only, (B) teeth-matching based on *weighted HD* of the effective contours only, and (C) a combination of method-B and DW-matching. Table 4 shows the retrieval accuracy for these

three methods. The results indicate that (1) the retrieval accuracy is better when matching all teeth in both jaws than matching in single jaw for all three methods, (2) matching based on *weighted HD* of the effective tooth contours (Method-B) is better than matching based on *HD* for the original contours (Method-A), and (3) matching using the combination of tooth contours and dental works is more effective than matching with only tooth contours. In addition to using tooth contour for image matching, the gain of using DW for matching is significant. This can be seen from Table 4 which indicates that Method-C can achieve 100% (35/35) retrieval accuracy while method-A and method-B can only achieve 74.3% (26/35) and 97.1% (34/35) accuracy, respectively, using top-2 retrievals.

5.4. Comparisons

We compare the identification accuracy of our proposed method with two other methods in Refs. [4,7], where the method in Ref. [4] is based on the tooth contour only and the method in Ref. [7] is based on both the tooth contours and the dental works. Although our method has higher retrieval accuracy rate, strictly speaking, we still cannot say that our method is absolutely superior to the other two methods because all three databases tested are different.

The method in Ref. [4] utilized two or three adjacent molar and pre-molar teeth together for queries and the traditional *HD* as the matching measurement. Among the 40 submitted PM bitewing images to be matched with the 102 AM bitewing images, the retrieval accuracy rate of the method in Ref. [4] is 82.5% (33/40) when using the top-1 retrieval and achieves 95% retrieval accuracy when using top-5 retrievals, which is lower than the result of our Method-B in Table 4 (94.3% (33/35) using the top-1 retrieval and 100% (35/35) using top-5 retrievals) but higher than the result of Method-A (68.6% (24/35) for the top-1 retrieval and 85.7% (30/35) for top-5 retrievals). The above comparison may favor our method, which is not quite fair to the other two methods because not all images in our testing database are genuine. However, we believe that the accuracy rates reveal certain level of powerfulness of our method.

The method in Ref. [7] utilized a pair of neighboring teeth as a unit for matching, in which the contours of teeth are matched based on the average distance of two contours after shape registration, the dental work is matched using the overlapping areas of the teeth, and these two matching scores are then combined for identification. Their database contains 235 AM images with 738 teeth and 166 PM images with 414 teeth belonging to different types of dental radiographs. For teeth matching, 95% of the genuine teeth were among top 8% (the first 59 ranks) of the retrievals, which is higher than our result of 87.3%=(87.8+86.7)/2 (approximately top-15) accuracy based on the weighted *HD* of the effective contour of a single tooth (Method-3 in Table 2). However, for image matching using both teeth and dental works, our Method-C in Table 4 achieves 100% accuracy in top 6% (the first 2 ranks out of 35) retrievals, which is in turn higher than their result of 90% accuracy using top 7% (the first 16 ranks out of 235) retrievals. Thus, it is obvious that our proposed image matching method gains its retrieval accuracy from using the dental work metrics in both spatial and frequency domains.

5.5. Discussion

The experimental results demonstrated that our proposed method can better handle the view variation problem for teeth matching and resolve the imperfect alignment of dental works using affine-transform invariant feature for dental work matching.

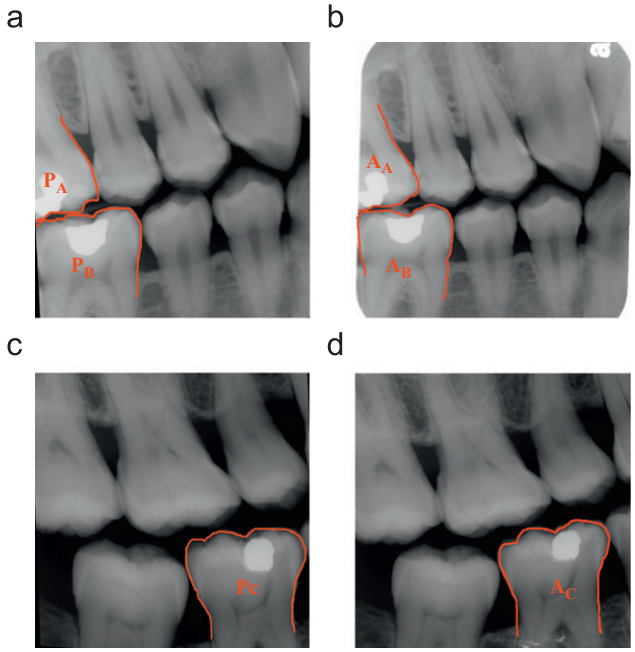

Fig. 10. Two failure cases of teeth matching. (a) PM, (b) AM, (c) PM, and (d) AM.

However, when only almost half of the tooth contours are available in both the query and the genuine database teeth, or either the query or the genuine database tooth misses a big portion of the contour, our proposed matching method still results in errors. As shown in Fig. 10(a)–(d), both $\mathbf{P_A}$ in (a) and $\mathbf{A_A}$ in (b) only have half of the contour, $\mathbf{P_B}$ in (a) misses the left side of contour against $\mathbf{A_B}$ in (b), and $\mathbf{P_C}$ in (c) misses some root information against $\mathbf{A_C}$ in (d). For such cases, our effective contour alignment method pruned the contour that has more edge information (e.g., $\mathbf{A_B}$ in (b) and $\mathbf{A_C}$ in (d)) to result in a better alignment; however, much important information for matching were also lost. Many teeth shapes that used to be vague in matching now become more similar, which leads to a reduction in retrieval accuracy. As in the cases of Fig. 10, the query teeth $\mathbf{P_A}$, $\mathbf{P_B}$, and $\mathbf{P_C}$ ineffectively retrieved the genuine database teeth $\mathbf{A_A}$, $\mathbf{A_B}$, and $\mathbf{A_C}$ at rank 24, 112, and 21, respectively.

6. Conclusion

We presented a dental identification method based on the contours of both teeth and dental works in bitewing radiographs. The contours of teeth are represented in a point series in spatial domain and the dental work contours are represented in both the spatial and the frequency domains. As the scale, orientation, and translation of PM and AM radiographs are generally different due to view and age variations, each tooth was firstly segmented and the query PM tooth was then aligned against the database AM tooth under matching using the best fit affine transformation. To reduce the alignment error caused from unreliable contours, we proposed a point-reliability measuring method and weighed each point based on its reliability when calculating the distance between two contours. To reduce the error caused from aligning two incomplete tooth contours, we proposed an outlier detection and pruning method and realigned the pruned contours so that the two can be aligned better for matching. Meanwhile, matching the spatial contours of dental works relies heavily on the wellness of tooth alignment and is sensitive to boundary disturbances; whereas matching with the affine-transform invariant Fourier descriptors will neglect the translation and orientation. Thus, we

proposed using a hybrid of both features to compensate the drawbacks of each other while keeping their advantages. Experiments showed that (1) the retrieval accuracy is better when matching all teeth in both jaws than in single jaw, (2) matching based on the weighted *HD* of the pruned tooth contours is better than the original contours, and (3) identification with a combination of tooth contours and dental works is more effective than identification with only tooth contours. Our future work includes applying teeth numbering method to identify each tooth as a specific one in the universal teeth number system. This will limit the search space to only including the teeth with the same assigned number and consequently improves the identification accuracy and speed.

Acknowledgments

The authors would like to thank the anonymous reviewers for their valuable comments and constructive suggestions. This research was supported by the National Science Council of ROC under grant # NSC 98-2221-E-126-009 and # NSC 99-2221-E-126-005.

References

[1] International Biometric Group's Biometrics Market and Industry Report 2009–2014. 〈http://www.biometricgroup.com/reports/public/market_report.php〉.
[2] G. Fahmy, D. Nassar, E. Haj-Said, H. Chen, O. Nomir, J. Zhou, R. Howell, H.H. Ammar, M. Abdel-Mottaleb, A.K. Jain, Toward an automated dental identification system (ADIS), Journal of Electronic Imaging 14 (2005) 1–13.
[3] P.L. Lin, Y.H. Yan, P.W. Huang, An effective classification and numbering system for dental bitewing radiographs using teeth region and contour information, Pattern Recognition 43 (2010) 1380–1392.
[4] J. Zhou, M. Abdel-Mottaleb, A content-based system for human identification based on bitewing dental X-ray images, Pattern Recognition 38 (2005) 2132–2142.
[5] O. Nomir, M. Abdel-Mottaleb, A system for human identification from X-ray dental radiographs, Pattern Recognition 38 (2005) 1295–1305.
[6] O. Nomir, M. Abdel-Mottaleb, Fusion of matching algorithms for human identification using dental X-ray radiographs, IEEE Transactions on Information Forensics and Security 3 (2008) 223–233.
[7] A.K. Jain, H. Chen, Matching of dental X-ray images for human identification, Pattern Recognition 37 (2004) 1519–1532.
[8] O. Nomir, M. Abdel-Mottaleb, Hierarchical contour matching for dental X-ray radiographs, Pattern Recognition 41 (2008) 130–138.
[9] M. Abdel-Mottaleb, O. Nomir, D.E. Nassar, G. Fahmy, H.H. Ammar, Challenges of developing an automated dental identification system, IEEE International Mid-west Symposium on Circuits and Systems 1 (2003) 411–414.
[10] H. Chen, A.K. Jain, Dental biometrics: alignment and matching of dental radiographs, IEEE Transactions on Pattern Analysis and Machine Intelligence 27 (2005) 1319–1326.
[11] M. Hofer, A.N. Marana, Dental biometrics: human identification based on dental work information, in: Proceedings of the XX Brazilian Symposium on Computer Graphics and Image Processing (2007) 281–286.
[12] O. Nomir, M. Abdel-Mottaleb, Human identification from dental X-ray images based on the shape and appearance of the teeth, IEEE Transactions on Information Forensics and Security 2 (2007) 188–197.
[13] E.H. Said, D.E.M. Nassar, G. Fahmy, H.H. Ammar, Teeth segmentation in digitized dental X-ray films using mathematical morphology, IEEE Transactions on Information Forensics and Security 1 (2006) 178–189.
[14] Y.H. Lai, P.L. Lin, Effective segmentation for dental X-ray images using texture-based fuzzy inference system, Advanced Concepts on Intelligent Vision Systems LNCS 5259 (2008) 936–947.
[15] J.F. Canny, A computational approach to edge detection, IEEE Transactions on Pattern Analysis and Machine Intelligence 8 (1986) 679–698.
[16] R. Gonzalez, R. Wood, Digital Image Processing 2/e, Prentice Hall, 2002.
[17] D.P. Huttenlocher, G.A. Klanderman, W.J. Rucklidge, Comparing images using the Hausdorff distance, IEEE Transactions on Pattern Analysis and Machine Intelligence 15 (1993) 850–863.
[18] C. Zhao, W. Shi, Y. Deng, A new Hausdorff distance for image matching, Pattern Recognition Letters 26 (2005) 581–586.
[19] V. Chandola, A. Banerjee, V. Kumar, Outlier Detection: A Survey, Technical Report, University of Minnesota, 2007.
[20] J. Fan, G. Zeng, M. Body, M. Hacid, Seeded region growing: an extensive and comparative study, Pattern Recognition Letters 26 (2004) 1139–1156.
[21] M. Mahoor, M. Abdel-Mottaleb, Classification and numbering of teeth in dental bitewing images, Pattern Recognition 38 (2005) 577–586.

Phen-Lan Lin received her BS degree in Engineering Science from the National Cheng-Kung University in 1973, both MSEE and Ph.D. degrees in Electrical Engineering from the Southern Methodist University, Dallas, Texas in 1992, and 1994, respectively. She is a professor in the Department of Computer Science and Information Engineering, Providence University since 2004, and had been a professor and an associate professor in the Department of Computer Science and Information Management in 1995–2003, as well as the Director of Computer and Communication Center in the university in 2002–2008. Prior teaching, Dr. Lin was with Texas Instruments in Dallas, Texas as a member of technical staff, lead engineer, and project manager from 1978 to 1992, respectively. Her current research interests include information security and privacy (including multimedia and network security), medical imaging, and automatic visual inspection.

Yan-Hao Lai received his BS degree in Information Management from the South Taiwan University in 2003. He earned his Ph.D. degree from the Department of Computer Science and Engineering of National Chung-Hsing University in 2011. His research interests include computer vision and information security.

Po-Whei Huang received his BS degree in applied mathematics from the National Chung-Hsing University in 1973, the MS degree in mathematics from the Texas Tech University in 1978, and the Ph.D. degree in computer science from the Southern Methodist University in 1989. He was with Texas Instruments in Dallas as a member of technical staff, project manager, and software development manager from 1978 to 1990. He was the department chairman and has been a professor in the Department of Computer Science and Engineering at National Chung-Hsing University. From September 2002 to October 2004, he served as the vice president of the National Formosa University located in Yunlin County of Taiwan. From October 2004 to January 2006, he was appointed as the Secretary General of National Chung-Hsing University. Since February 2006, he has been the dean of College of Science at National Chung-Hsing University. He is a fellow of IET and distinguished professor of National Chung-Hsing University. His research interests include image database, computer vision, pattern recognition, and image processing.